

Point-contact spectroscopy of Al- and C-doped MgB₂. Superconducting energy gaps and scattering studies.

P. Szabo,¹ P. Samuely,¹ Z. Holánová,¹ S. Bud'ko,² P. C. Canfield,² and J. Marcus³

¹Centre of Low Temperature Physics, IEP Slovak Academy of Sciences &

P. J. Safarik University, Watsonova 47, SK-04001 Košice, Slovakia

²Ames Laboratory and Iowa State University, Ames, IA 50011, USA

³LEPES CNRS, F-38042 Grenoble Cedex 9, France.

(dated: January 13, 2022)

The two-band/two-gap superconductivity in aluminium and carbon doped MgB₂ has been addressed by the point-contact spectroscopy. Two gaps are preserved in all samples with T_c's down to 22 K. The evolution of two gaps as a function of the critical temperature in the doped systems suggest the dominance of the band-filling effects but for the increased Al-doping the enhanced interband scattering approaching two gaps must be considered. The magnetic field dependences of the Andreev reflection excess currents as well as zero-energy density of states determined from the experimental data are used to analyze the intraband scattering. It is shown, that while the C-doping increases the intraband scattering in the σ -band more rapidly than in the π -band, the Al-doping does not change their relative weight.

PACS numbers: 74.50.+r, 74.60.Ec, 74.72.-h

I. INTRODUCTION

Magnesium diboride owes its high critical temperatures of 40 K [1] to the interplay between two distinct electronic bands crossing the Fermi level. About half of the quasiparticles belongs to the quasi two-dimensional hole band and the Cooper pairs there are strongly coupled via the boron vibrational mode E_{2g}. The rest of the quasiparticles resides in the three-dimensional band with a rather moderate electron-phonon interaction. Without the effect from the σ -band the transition temperature T_c would be just a fraction of those found in the real MgB₂ [2, 3]. The two band superconductivity is the most spectacularly revealed by the presence of two very distinguished energy gaps, large in the σ and small in the π bands [4, 5, 6, 7, 8]. Superconducting properties of such a system are sensitive to the scattering. Due to coexistence of charge carriers from two almost completely separated bands two intraband and one interband scattering channels have to be distinguished. The interband scattering by non magnetic scatterers is supposed to have a particularly strong effect in a two-band superconductor: it will blend the strongly and weakly coupled quasiparticles, merge two gaps and consequently decrease T_c. In the case of MgB₂ T_c can drop down to about 20 K [3]. Fortunately, a different symmetry of the bands ensures that the interband scattering remains small also in very dirty MgB₂ samples which show about the same T_c as the purest material [9]. A systematic decrease of T_c is achieved in substituted MgB₂ samples. The only on-site substitutions by non magnetic elements which are known so far are carbon for boron and aluminium for magnesium. The carbon and aluminium atoms in MgB₂ take indeed a role of scatterers but they also dope the system with one extra electron which inevitably leads to the filling effect in the σ -band, with strongly coupled holes. Recently, Kortus et al. [10] have introduced a model in-

corporating both effects: interband scattering and band filling in MgB₂. The former effect leads to an increase of the small gap and decrease of the large σ while the latter suppresses both σ and π . There is a rather controversial situation as far as the strength of both effects in the Al and C-doped MgB₂ is concerned [10, 11].

In contrast to the interband scattering an increase of the scattering within the bands does not have any effect on the two gaps. But, the selective tuning of the intraband scattering can lead to the expressive variation of the values of the upper critical magnetic field H_{c2}(0) and its anisotropy [12, 13]. Upon increased C-doping H_{c2}(0) is increased significantly in both principal crystallographic directions (parallel to the ab hexagonal boron layers and the c-axis direction). On the other hand Al substitution suppresses H_{c2}(0) in the ab-plane direction and in the c-axis direction H_{c2} is hardly changed. This difference behavior is due to a different influence of C- and Al-doping on intraband scatterings. While the strong increase of H_{c2}(0) with the C-doping is due to graded dirty limit conditions, Al-doped samples stays still in the clean limit and the decrease of H_{c2} is just a consequence of the lower T_c [12]. A weight of scatterings in separated bands is still not clear.

In this paper we present the systematic study of the superconducting energy gaps in both Al- and C-doped magnesium diboride systems at stoichiometries Mg_{1-x}Al_xB₂ with x = 0; 0.1 and 0.2 and Mg(B_{1-y}C_y)₂ with y = 0; 0.021; 0.038; 0.055; 0.065 and 0.1. For the carbon doping this work is a supplement to our previous studies [14] on Mg(B_{1-y}C_y)₂ with y = 0; 0.021; 0.038; and 0.1. The influence of both substitutions for the scattering processes is discussed.

II. EXPERIMENT

Polycrystalline samples of Al-doped MgB_2 have been prepared by a two step synthesis at high temperatures as $\text{Mg}_{0.8}\text{Al}_{0.2}\text{B}_2$ and $\text{Mg}_{0.9}\text{Al}_{0.1}\text{B}_2$ with $T_c = 30.5\text{ K}$ and 23.5 K , resp. [12]. The carbon substituted samples $\text{Mg}(\text{B}_{1-y}\text{C}_y)_2$ with $y = 0; 0.055; 0.065; 0.1$ and with the respective transitions at $T_c = 39\text{ K}, 33\text{ K}, 28.2\text{ K}$, and 22 K , were synthesized in the form of pellets following the procedure described in Ref.[12] from magnesium lumps and B_4C powder. For $y = 0; 0.021; 0.038$ we have worked with the wire segments with $T_c = 39\text{ K}, 37.5\text{ K}$, and 36.2 K [15]. The undoped MgB_2 sample with $T_c = 39\text{ K}$ in a dirty limit with the high upper critical field has been prepared from boron and magnesium powder as described elsewhere [4].

The point-contact (PC) measurements have been realized via the standard lock-in technique in a special point-contact approaching system with lateral and vertical movements of the PC tip by a differential screw mechanism. The microconstrictions were prepared in situ by pressing different metallic tips (copper and platinum) formed either mechanically or by electrochemical etching) on different parts of the freshly polished surface of the superconductor. Point-contact measurements on the wire segments have been performed in a "reversed" configuration – with the $\text{Mg}(\text{B}_{1-x}\text{C}_x)_2$ wire as a tip touching softly a bulk piece of electrochemically cleaned copper. T_c 's in both series of substitutions have been determined from the resistive transitions and also from the temperature dependences of the point-contact spectra. The transition temperatures found by both methods were essentially the same, indicating that the information obtained from a more surface sensitive point-contact technique is relevant also for the bulk.

The point-contact spectrum measured on the ballistic microconstriction between a normal metal (N) and a superconductor (S) consist of the Andreev reflection (AR) contribution and the tunneling contribution [16]. The charge transfer through a barrierless metallic point-contact is realized via the Andreev reflection of carriers. Consequently at $T = 0$ the PC current as well as the PC conductance inside the gap voltage ($V < \pm e$) is twice higher than the respective values at higher energies ($V \gg \pm e$). The presence of the tunneling barrier reduces the conductance at the zero bias and two symmetrically located peaks rise at the gap energy. The evolution of the point-contact spectra between the pure Andreev reflection and the Gaver-like tunnelling case has been theoretically described by the Blonder-Tinkham-Klapwijk (BTK) theory [16]. The point-contact conductance data can be compared with this theory using as input parameters the energy gap Δ , the parameter z (measure for the strength of the interface barrier) and a parameter Γ for the spectral broadening [17]. In any case the voltage dependence of the N/S point-contact conductance gives direct spectroscopic information on the superconducting order parameter Δ . For the two-gap MgB_2

superconductor the point-contact conductance G can be expressed as a weighted sum of two partial BTK conductances: those from the quasitwo-dimensional σ -band (with a large gap Δ_σ) and those from the 3D π -band (with a small gap Δ_π)

$$G = G_\sigma + (1 - \alpha)G_\pi : \quad (1)$$

The weight factor α for the σ -band contribution can vary from 0.6 for the point-contact current strictly in the MgB_2 ab-plane to 0.99 of c-axis direction [18].

III. RESULTS AND DISCUSSION

A. Zero field point-contact spectroscopy

A large number of the point-contact measurements have been performed on the tested samples of pure MgB_2 and both substituted series. The point contacts revealed different barrier transparencies changing from more metallic interfaces to intermediate barriers with $0.4 < z < 0.8$ for the aluminum doped series and $0.4 < z < 1.2$ for the C-doped samples. By trial and error we looked for the spectra showing both gaps of a polycrystalline specimen. For more detailed studies we chose those junctions revealing the spectra with a low spectral broadening, i.e. with an intensive signal in the normalized PC conductance. As a result we succeeded to obtain many point contact spectra with well resolved two superconducting gaps directly in the raw data for all of the studied substitutions except for the highest dopings, $\text{Mg}_{0.8}\text{Al}_{0.2}\text{B}_2$ and $\text{Mg}(\text{B}_{0.9}\text{C}_{0.1})_2$. Figure 1 displays the representative spectra of the aluminum doped series and Fig. 2 resumes the results for the carbon doped MgB_2 . The experimental data are presented by the full lines, while the fits to the two-gap formula are indicated by the open circles. All shown point-contact spectra have been normalized to the spectra measured in the normal state at a temperature above T_c . The upper curves are shifted for the clarity. The retention of two gaps for all dopings apart from the highest substitution is evident.

For the highest dopings (always with a larger spectral broadening, $\Gamma \approx 0.2$), the spectra in Figs. 1 and 2 reveal only one pair of peaks without an apparent shoulder at the expected position of the second gap. For those data measured at 1.6 K (the rest of the data was measured at 4.2 K) also the one-gap fit is presented. The one-gap fit can reproduce either the height of the peaks or the width of them, while the two-gap fit can reproduce both. The size of the apparent gap is well indicated by the peak position, which is about 2 meV for $\text{Mg}_{0.8}\text{Al}_{0.2}\text{B}_2$ and 1.6 meV for $\text{Mg}(\text{B}_{0.9}\text{C}_{0.1})_2$. But, this size is too small to explain the superconductivity with the respective T_c 's equal to 23.5 K and 22 K within the single-gap BCS scenario suggesting, that we are dealing with a smeared two-gap structure. In the case of the 10% C-doped MgB_2 an existence of the large gap was clearly shown by the specific heat measurements [19]. Moreover, an existence of

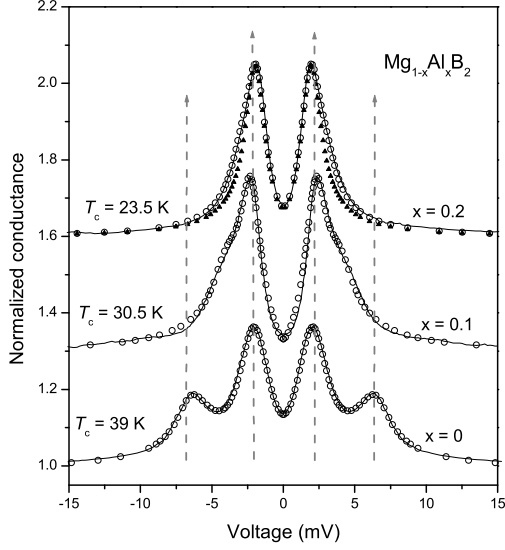


FIG. 1: Normalized point-contact spectra on $\text{Mg}_{1-x}\text{Al}_x\text{B}_2$ with $x = 0, 0.1$ and 0.2 —solid lines. Symbols show the fitting curves: open circles for the two-gap BTK model and solid triangles for the one-gap BTK model. The spectra are vertically shifted for the clarity. The dashed vertical arrows emphasize the tendency of the evolution of the gaps.

the both gaps was strongly evidenced in a single experiment by our previous point-contact spectroscopy measurements in applied magnetic field [14]. There, the spectrum at $H = 0.7 \text{ T}$ showed that the contribution from the

band was partially suppressed and the large-gap shoulder clearly appeared near 3 mV besides the gap peak at 1.6 mV . A similar effect has the magnetic field in the case of 20% Al doped MgB_2 : As shown in the top panel of Fig. 5, the peak position being at about 2 mV in zero field, is shifted towards 3 mV at 1 Tesla . In the case of a single-gap superconductor the application of magnetic field can only lead to a shrinkage of the distance between the peak positions in the point-contact spectrum. It is a simple consequence of an introduction of the vortices and magnetic pair-breaking [20]. The shift of the peak of the PC spectra to higher voltages demonstrated in Fig. 5 is then due to an interplay between the two gaps, because the dominance of the peak at zero field is suppressed in increasing field and contributes more. Thus, the retention of two gaps is proved in the all presented doped MgB_2 samples with T_c 's from 39 down to 22 K .

The statistics of the energy gaps obtained from fitting to the two-band BTK formula is shown in Fig. 3, for each C and Al concentration. The left coordinates indicate the transition temperature of the junctions, while the right one counts the number of junctions with the same size of the gaps. The energy width of a particular count indicates the fitting uncertainty. All the samples, the undoped MgB_2 as well as the aluminum and car-

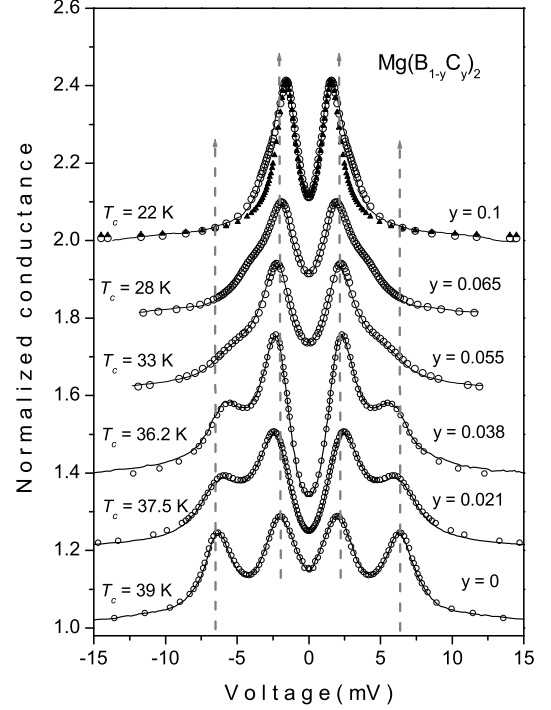


FIG. 2: Normalized point-contact spectra measured on $\text{Mg}(\text{B}_{1-y}\text{C}_y)_2$ with $y = 0, 0.021, 0.038, 0.055, 0.065$ and 0.1 —solid lines. Symbols show the fitting curves: open circles for the two-gap BTK model and solid triangles for the one-gap BTK model. The spectra are vertically shifted for the clarity. The dashed vertical arrows emphasize the tendency of the evolution of the gaps.

bon doped material reveal a certain distribution of the small and large gaps but the two gaps are well distinguishable in the histogram and no overlap of and is observed. Already from this figure a general tendency is evident, namely that the reduction of the large gap is proportional to the decreasing transition temperature. On the other hand the changes in the small gap are proportionally smaller.

Figure 4 displays the energy gaps as a function of T_c 's. The points (open squares for Al dopings and solid circles for C ones) are positioned at the averaged energies of the gap distributions from Fig. 3 and the error bars represent the standard deviations. The large gap is essentially decreased linearly with the respective T_c 's. The behavior of 's is more complicated. For both kind of substitutions the gap is almost unchanged at smaller dopings. In the case of C-doped MgB_2 it holds clearly down to $T_c = 33 \text{ K}$. In $(\text{MgAl})\text{B}_2$ of the 10% Al doped sample seems to even slightly increase. But for the highest dopings decreases in both doping cases. The dashed lines in Fig. 4 are calculations of Kortus et al. [10] for the case of a pure band filling effect and no

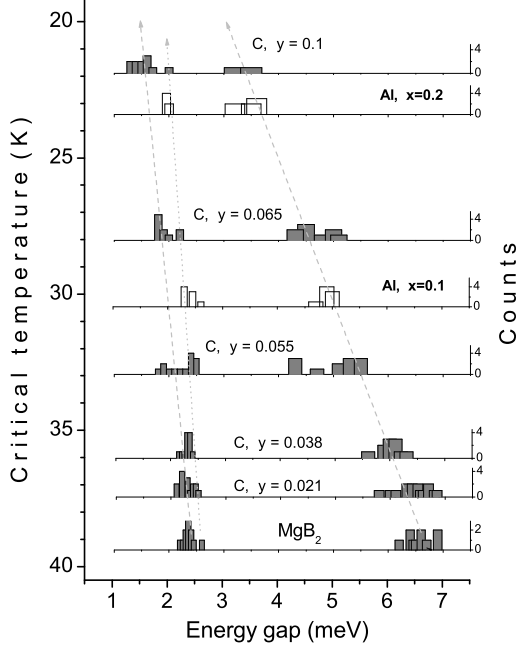


FIG. 3: Distribution of the superconducting energy gaps of $\text{Mg}(\text{B}_{1-y})\text{C}_y)_2$ – gray columns and $\text{Mg}_{1-x}\text{Al}_x\text{B}_2$ – open columns. The dashed and dotted lines are guides for the eyes.

interband scattering. Although, the constant γ is not reproduced, the T_c dependence of γ 's for carbon doping are broadly well described. The solid lines show the Kortus's calculations including the interband scattering with the rate $\tau_{IB} = 1000\text{ps}$ (or 2000ps). As can be seen the gaps in the Al-doped samples cannot be accounted without an interband scattering but it is smaller than in the presented calculations.

Recently, similar results on the superconducting energy gaps have been obtained on the Al-doped single crystals by some of us and other authors [21] exploring the specific heat as well as the point contact spectroscopy measurements. Those data also show a tendency of approaching of the two gaps with their possible merging in the Al-doped samples with T_c below 10-15 K. It is worth noticing that those and here presented results do not show any decrease of the large gap below the canonical BCS value for the Al-doped MgB_2 with T_c 's below 30 K found earlier [22].

For the carbon doped samples we have not found any stronger tendency to blend both gaps down to $T_c = 22\text{K}$, being in contrast with the data obtained on single crystals by Gonnelli et al. [23]. On the other hand our data are very compatible with the recent ARPES measurements of Tsuda et al. where both gaps have been directly seen in the raw data down to T_c of 23 K. A presence of two gaps is also evidenced by the point contact measurements of Schmidt et al. [24] on the heavily carbon doped MgB_2 .

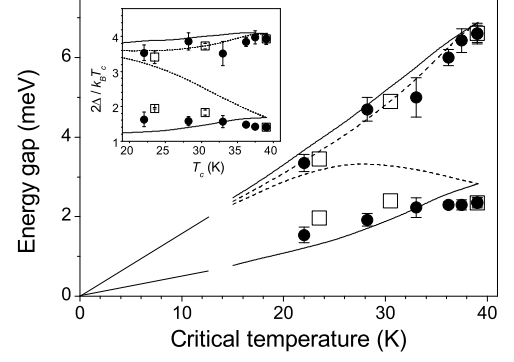


FIG. 4: Averaged values of the superconducting energy gaps as a function of the critical temperatures of $\text{Mg}(\text{B}_{1-y})\text{C}_y)_2$ – solid circles and $\text{Mg}_{1-x}\text{Al}_x\text{B}_2$ samples – open squares. The error bars represent the standard deviations in the distribution shown in Figure 3. The lines – see the text.

We remark that the data showing no merging of the gaps on the heavily doped MgB_2 with T_c down to 22 K have been collected from the measurements on the samples of different forms (wires, sintered pellets, polycrystals) prepared by different methods. Moreover it is very important that two gaps have been directly experimentally evidenced in the raw data without any dependence on the model or fit.

The theoretical calculations of Erwin and Mazin [25] on merging of the gaps due to a substitution are also supporting the picture presented here. By them the carbon substitution on the boron site should have zero effect on the merging of the gaps. It is due to the fact that a replacing boron by carbon does not change the local point symmetry in the σ and π orbitals which are both centered at the boron sites. Then, the interband scattering is of little probability without incorporating extra defects producing a change of the symmetry of orbitals. On the other hand much bigger effect is expected for the out of plane substitutions (Al instead of Mg) or defects which would indeed change the local point symmetry. The substitution of Al instead of Mg leads also to a significant decrease of the c-lattice parameter [26] (it is basically null in case of carbon doping), which helps the inter-layer hopping from a p_z orbital (π -band) in one atomic layer to a σ bond orbital in the next one. Of course, a particular strength of the interband scattering can scatter among samples due to defect and thus the merging of two gaps could be sample dependent.

B. Magnetic field effects

In the following we present the effect of magnetic field on the point contact spectra of the aluminum as well

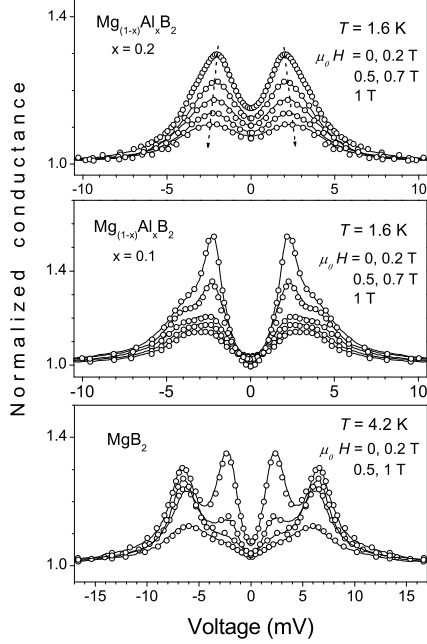


FIG. 5: Influence of the applied magnetic field on the point-contact spectra of $\text{Mg}_{1-x}\text{Al}_x\text{B}_2$ – solid lines. Open circles show fitting results for the two-band mixed state BTK formula.

as carbon doped MgB_2 samples. The field effect has been measured on a number of samples of each substitution. The field was always oriented perpendicularly to the sample surface and parallel with the tip having the point contact area in the vortex state.

Figure 5 displays the typical magnetic field dependences of the PC spectra (lines) obtained on $\text{Mg}_{1-x}\text{Al}_x\text{B}_2$ samples with $x = 0, 0.1$ and 0.2 . The zero-field spectrum of the undoped MgB_2 (bottom panel) reveals an expressive two-gap structure. At small fields the peak corresponding to the small gap is very rapidly suppressed and only the peak responsible for the large gap is apparently visible above 1 Tesla. At 10 % of Al doping the zero field spectra also show both gaps but the large one is now revealed more as a pronounced shoulder. Again at a small magnetic field the γ -band-gap peak is rapidly suppressed but its signature is still distinguishable at 0.5 Tesla. At higher fields the signatures of both gaps are not resolvable due to an interference of the related peaks placed at closed positions. The resulting maximum is located in the intermediate position between them. At the highest doping (20 % Al) such an interference of even closer gaps is graduated, so already at zero magnetic field one can see only one pair of peaks at the position of the small gap (it has always much higher weight at zero field) and a minor shoulder at the voltage of the large one. In the increasing field the peak

is broadened and its position shifted to higher voltages (indicated by arrows). As mentioned above the shift is an indication of two gaps present in the spectrum with an increasing weight of the large-gap peak with respect to the small one.

The in-field measurements have also been performed on the carbon doped samples. In our previous paper [14] they have been demonstrated on the heavily doped, 10 % C MgB_2 sample.

In two sets of measurements and subsequent analysis on the aluminum and carbon doped samples two different types of undoped MgB_2 samples have been used. The carbon doping increases the upper critical fields [12] despite the decreased T_c and both superconducting gaps. Thus, these samples are driven to the dirty limit by doping. That is why we compare the 6.5 % and 10 % C-doped samples with the undoped MgB_2 crystal being already in a dirty limit ($T_c = 39 \text{ K}$, $H_{c2\parallel\text{jjc}} = 5 \text{ T}$) [4]. On the other hand the aluminum doping leads only to a decrease of H_{c2} for the field in ab planes or a constant value in perpendicular orientation with $H_{c2\parallel\text{jjc}} = 3 \text{ T}$ [12], so we have chosen the pure MgB_2 sample with $T_c = 39 \text{ K}$ and $H_{c2\parallel\text{jjc}} = 3 \text{ T}$ as a reference.

From the in-field spectra the excess current I_{exc} has been determined. It was calculated by integrating the PC spectra after subtracting an area below unity. When a single gap superconductor is in the vortex state, each vortex core represents a normal state region and this region/vortex density increases linearly up to the upper critical magnetic field. Thus, the PC excess current (I_{exc}) is reduced linearly in increasing magnetic field by the factor of $(1 - n)$, where n represents a normal state region – the PC junction area covered by the vortex cores. The field dependences of the excess currents I_{exc} obtained on the carbon and aluminum doped samples are shown in Fig. 6a and 6b, respectively. The magnetic field coordinates have been normalized to an appropriate $H_{c2\parallel\text{jjc}}$ referred to as $h = H/H_{c2\parallel\text{jjc}}$ [27]. In a none case the linear decrease of I_{exc} was observed. On the contrary, a strong non-linearity observed in all curves approves a presence of two gaps in the quasiparticle spectrum of the material. There, a more rapid fall of $I_{\text{exc}}(h)$ at low magnetic fields is ascribed to a strong filling of the γ -band gap states up to a virtual/crossover γ -band upper critical field $H_{c2\parallel\text{jjc}}^{\gamma}$. Then, at higher fields, the low temperature superconductivity is maintained mainly by the γ -band [29], with the γ gap getting filled smoothly up to the real upper critical field of the material $H_{c2} = H_{c2\parallel\text{jjc}}^{\gamma}$. Due to a small, but finite coupling of the two bands, the superconductivity is maintained also in the γ -band above $H_{c2\parallel\text{jjc}}^{\gamma}$, but, as shown e.g. in the tunneling data of Eskildsen et al. [28], the γ -gap states are filled much more slowly than in the low field region. A magnitude of the upper critical fields of two bands can be estimated in the clean limit [30] as $H_{c2\parallel\text{jjc}}^{\gamma} = \frac{2}{\sqrt{2}} v_F^2$ and $H_{c2\parallel\text{jjc}} = \frac{2}{\sqrt{2}} v_F^2$, with v_F or v_F^{γ} for the Fermi velocity of the respective band (since only $H_{c2\parallel\text{jjc}}$ is considered the anisotropy due to an effective mass tensor is neglected).

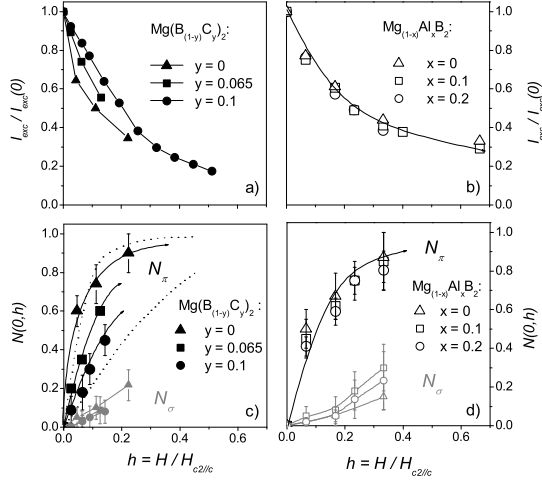


FIG. 6: a) Excess currents $I_{\text{exc}}(h)$ of $\text{Mg}(\text{B}_{(1-y)}\text{C}_y)_2$. b) $I_{\text{exc}}(h)$ of $\text{Mg}_{1-x}\text{Al}_x\text{B}_2$. c) Zero-bias density of states $N(0;h)$ of $\text{Mg}(\text{B}_{(1-y)}\text{C}_y)_2$. d) Zero-bias DOS of $\text{Mg}_{1-x}\text{Al}_x\text{B}_2$ determined from the fitting for the two-band mixed state BTK formula. The solid lines are guides for the eyes. All here presented field dependencies have been determined from the point-contact spectra with similar weight of the π -band contribution ≈ 0.75 – 0.05 . The dotted and dashed gray lines in Fig. 6c represents the theoretical predictions of Ref. [33] for the dirty MgB_2 samples with the ratio of in-plane diffusivities $D_{\parallel}/D_{\perp} = 0.2$ and 1 , respectively.

A similar estimates can be done in the dirty limit when taking into account the respective diffusion coefficients $D_{\parallel}(\gamma) : H_{c2}; (\gamma) = D_{\perp}(\gamma)$.

Fig. 6a shows that the carbon doping leads to changes in the field dependence of the excess current. The undoped MgB_2 reveals a very steep fall of I_{exc} already at small fields indicating also proportionally small crossover field $H_{c2};$. By doping the π -band crossover field apparently shifts to higher values. From the previous subsection we know that the carbon doping does not influence significantly the interband scattering in MgB_2 . The ratio between the two gaps, $\Delta_{\pi}/\Delta_{\sigma}$ remains almost unchanged. Then, following from the dirty limit theory the shift of the normalized crossover field $H_{c2}; = H_{c2}/H_0$ is due to an increase of the ratio of the diffusion coefficients D_{\parallel}/D_{\perp} . This is an indication that the carbon doping leads to a significant enhancement of the π -band scattering.

In Fig. 6b the excess currents on the aluminum doped samples show different picture: there is no change in the field dependence of I_{exc} upon the aluminum doping up to 20 % indicating constant value of the crossover field $H_{c2};$. Qualitatively, it can be understood in the framework of the clean limit persisting in the Al-doped MgB_2

up to 20 % Al doping region. Indeed, the constant value of the upper critical field $H_{c2};$, which is equal to approximately 3 Tesla for all three dopings, indicates the constant ratio between Δ_{π} and v_F . It means that the electron filling of the hole π -band decreases both quantities proportionally. Then, $H_{c2};$ must be only weakly doping dependent. As $H_{c2};^2 = v_F^2$, and Δ_{π} remains almost constant for $x = 0.1$ and 0.2 this would suggest that v_F remains also unchanged.

Quantitatively, I_{exc} of the two-gap superconductor in the mixed state can be described by the sum [31]

$$I_{\text{exc}} = (1 - n_{\pi}) + (1 - n_{\sigma})(1 - n_{\pi}) : (2)$$

For the point-contact conductance a similar expression can be written

$$G = [n_{\pi} + (1 - n_{\sigma})G] + (1 - n_{\pi})[n_{\sigma} + (1 - n_{\sigma})G] : (3)$$

Considering that n_{π} and n_{σ} represent independent fillings of the respective gaps in increasing applied field, their values can be identified with the values of the zero-energy density of states $N(0;H)$ and $N(0;H)$ averaged over the vortex lattice. This model proposed by Bugoslavsky et al. [32] enables a direct experimental determination of the field dependent energy gaps and zero-energy DOS $N(0;H)$ from the point-contact spectra in MgB_2 . The calculations of Koshelev and Golubov [33] show that the low field slope of $N(0;H)$ is controlled by an important parameter D_{\parallel}/D_{\perp} which can thus be established.

Unfortunately the fitting of the PC conductance of MgB_2 in the mixed state is not trivial because of too many (9) parameters. Moreover two pairs of the parameters N_{π} vs. Δ_{π} and N_{σ} vs. Δ_{σ} manifest very similarly in the fit. Hence, before fitting the spectra by the formula (3) we estimate $N(0;H)$ values from the excess currents. Here some simplifications were made: If the real upper critical field H_{c2} is large compared to $H_{c2};$, in the region $0 < H < H_{c2};$ the suppression of the π -band contribution by the field can be neglected ($N(0;H) = 0$). If we also neglect a small reduction of the energy gaps at these fields [32, 35], then $I_{\text{exc}}(H)$ can be represented by a single parameter formula expressed as $I_{\text{exc}} / (1 - N(0;H)) = (0) + (1 - (0)) (0)$ since all other parameters (0) , (0) and (0) have already been determined from the BTK fit at $H = 0$. The resulting $N(0;H)$ is later used as a first approximation in the fit of the PC conductance spectrum. There, also the values of $z_{\pi}; z_{\sigma}$ and $\Delta_{\pi}; \Delta_{\sigma}$ determined from BTK fits at $H = 0$ are kept unchanged. In the second step all parameters except for $z_{\pi}; z_{\sigma}$ and $\Delta_{\pi}; \Delta_{\sigma}$ are adjusted for the best fit. The resulting values of $N(0;H)$ are decreased by 5–20% in comparison with the first estimate from $I_{\text{exc}}(H)$ [34]. Also the values of the smearing parameters Δ_{π} and Δ_{σ} reveal about 10%–20% of increase in the interval $0 < H < 1$ T accounting for the magnetic pair-breaking of the superconducting DOS. In the same field interval a small (5–10%) suppression of the values of the energy gaps has been obtained.

The resulting zero-energy DOS $N(0;h)$ and $N(0;h)$ are plotted in Fig.6c for the carbon-doped samples and in Fig.6d for the Al-substituted MgB_2 . Again, the carbon and aluminum dopings reveal very differently. The steep increase of $N(0;h)$ in the undoped MgB_2 can be ascribed within the framework of the dirty superconductivity model [33] to a small value of the ratio of in-plane diffusivities $D_{\parallel}/D_{\perp} < 1$ (see dotted line, calculated for $D_{\parallel}/D_{\perp} = 0.2$). It means a dirtier γ -band than the σ -one. The subsequent decrease of the low field slope of $N(0;h)$ upon C-doping can be explained by an increase of the D_{\parallel}/D_{\perp} ratio, i.e. by a more rapid enhancement of the γ -band intraband scattering as compared with the scattering in the σ -band. The dashed line plots the theoretical $N(0;h)$ dependence at $D_{\parallel}/D_{\perp} = 1$.

The situation is different for the Al-doping. Here the field dependences of $N(0;h)$ reveal no change upon doping. The same explanation as used above for the excess current versus field can be applied, underlying the conservation of the superconducting clean limit for Al-doping.

IV. CONCLUSIONS

The influence of carbon and aluminum doping on the two-band/two-gap superconductivity in MgB_2 has been studied by the point-contact spectroscopy. It has been

shown, that the decreased transition temperatures and the evolution of the gaps upon both substitutions is mainly a consequence of the band filling effect. However, in the case of an increased Al-doping also an increase of the interband scattering has to be taken into account. By the analysis of the field dependences of the point-contact spectra we have shown, that the C-doping increases the scattering in the γ -band more rapidly than in the σ -one. On the other hand, the Al-doping does not introduce significant changes in the relative weight of the scatterings within two bands.

Acknowledgments

This work has been supported by the Slovak Science and Technology Assistance Agency under contract No. APVT-51-016604. Centre of Low Temperature Physics is operated as the Centre of Excellence of the Slovak Academy of Sciences under contract no. I/2/2003. Ames Laboratory is operated for the U.S. Department of Energy by Iowa State University under Contract No. W-7405-Eng-82. This work was supported by the Director for Energy Research, Office of Basic Energy Sciences. The liquid nitrogen for the experiment has been sponsored by the U.S. Steel Kosice, s.r.o.

-
- [1] J. Nagamatsu, N. Nakagawa, T. Muranaka, Y. Zenitani, J. Akimitsu, *Nature (London)* 410, 63 (2001).
 - [2] A. Y. Liu, I. I. Mazin, and J. Kortus, *Phys. Rev. Lett.* 87, 087005 (2001).
 - [3] H. J. Choi, D. Roundy, H. Sun, M. L. Cohen, and S. G. Louie, *Nature* 418, 758 (2002); H. J. Choi, D. Roundy, H. Sun, M. L. Cohen, and S. G. Louie, *Phys. Rev. B* 66, 020513 (2002).
 - [4] P. Szabo, P. Samuely, J. Kacmarcik, T. Klein, J. Marcus, D. Fruchart, S. Miraglia, C. Marcenat, and A. G. M. Jansen, *Phys. Rev. Lett.* 87, 137005 (2001).
 - [5] F. Gubileo, D. Roditchev, W. Sacks, R. Lamy, D. X. Thanh, J. Klein, S. Miraglia, D. Fruchart, J. Marcus, and Ph. Monod, *Phys. Rev. Lett.* 87, 177008 (2001).
 - [6] M. Iavarone, G. Karapetrov, A. E. Koshelev, W. K. Kwok, G. W. Crabtree, D. G. Hinks, W. N. Kang, E.-M. Choi, H. J. Kim, H.-J. Kim, and S.-I. Lee, *Phys. Rev. Lett.* 89, 187002 (2002).
 - [7] P. Martinez-Samper, J. G. Rodrigo, G. Rubio-Bollinger, H. Suderow, S. Vieira, S. Lee, and S. Tajima, *Physica C* 385, 233 (2003).
 - [8] S. T. Suda, T. Yokoya, Y. Takano, H. Kito, A. Matsushita, F. Yin, J. Itoh, Harima, and S. Shin, *Phys. Rev. Lett.* 91, 127001 (2003).
 - [9] I. I. Mazin, O. K. Andersen, O. Jepsen, A. A. Golubov, O. V. Dolgov, and J. Kortus, *Phys. Rev. B* 69, 056501 (2004).
 - [10] J. Kortus, O. V. Dolgov, R. K. Kramers, and A. A. Golubov, *Phys. Rev. Lett.* 94, 027002 (2005).
 - [11] P. Samuely, P. Szabo, P. C. Canfield, and S. L. Bud'ko, *Phys. Rev. Lett.* 95, 099701 (2005).
 - [12] M. Angst, S. L. Bud'ko, R. H. T. Wilke and P. C. Canfield, *Phys. Rev. B* 71, 144512 (2005).
 - [13] A. Gurevich, *Phys. Rev. B* 67, 184515 (2003).
 - [14] Z. Holanová, P. Szabo, P. Samuely, P. C. Canfield, and S. L. Bud'ko, *Phys. Rev. B* 70, 064520 (2004); P. Samuely, Z. Holanová, P. Szabo, J. Kacmarcik, P. C. Canfield and S. L. Bud'ko, *Phys. Rev. B* 68, 020505 (R) (2003).
 - [15] R. H. T. Wilke, S. L. Bud'ko, P. C. Canfield, D. K. Finnemore, R. J. Suplinskas and S. T. Hannahs, *Phys. Rev. Lett.* 92, 217003 (2004).
 - [16] G. E. Blonder, M. Tinkham, T. M. Klapwijk, *Phys. Rev. B* 25, 4515 (1982).
 - [17] A. P. Leenik, M. G. Rajcar, S. Benacka, P. Seidel, and A. P. Ficht, *Phys. Rev. B* 49, 10016 (1996).
 - [18] A. Brinkman, A. A. Golubov, H. Rogalla, O. V. Dolgov, J. Kortus, Y. Kong, O. Jepsen, and O. K. Andersen, *Phys. Rev. B* 65, 180517 (R) (2002).
 - [19] R. A. Ribeiro, S. L. Bud'ko, C. Petrovic, and P. C. Canfield, *Physica C* 384, 227 (2003).
 - [20] P. Samuely, P. Szabo, J. Kacmarcik, T. Klein, *Physica C* 385, 244 (2003).
 - [21] T. Klein, L. Lyard, J. Marcus, C. Marcenat, P. Szabo, Z. Holanová, P. Samuely, B. Kang, H.-J. Kim, H.-S. Lee and S. I. Lee, to be published.
 - [22] M. Putti, C. Ferdeghini, M. Monni, I. Palleschi, C. Tarantini, P. Manfrinetti, A. Palenzona, D. Daghero, R. S. Gonnelli and V. A. Stepanov, *Phys. Rev. B* 71, 144505 (2005).

- [23] R. S. Gonnelli, D. Daghero, A. Calzolari, G. A. Ummarino, V. Dellarocca, V. A. Stepanov, S. M. Kazakov, N. Zhigadlo and J. Karpinski Phys. Rev. B 71, 060503 (2005).
- [24] H. Schmidt, K. E. Gray, D. G. Hinks, J. F. Zasadzinski, M. Avdeev, J. D. Jorgensen, and J. C. Burley, Phys. Rev. B 68, 060508 (R) (2003).
- [25] S. C. Erwin and I. I. Mazin, Phys. Rev. B 68, 132505 (2003).
- [26] M. Putti, M. Afronte, P. Manfrinetti, and P. Palenzona, Phys. Rev. B 68, 094514 (2003).
- [27] Due to measurements on polycrystals the field orientation is not fully controlled. But in the present study we are interested mainly in the behavior of the isotropic band, thus the choice of the crystallographic orientation of the "reference" upper critical field is arbitrary but once chosen it must be kept for all compared doped samples.
- [28] M. R. Eskildsen, M. Kugler, S. Tanaka, J. Jun, S. M. Kazakov, J. Karpinski, and O. Fischer, Phys. Rev. Lett. 89, 187003 (2002).
- [29] V. G. Kogan and S. L. Bud'ko, Physica C 385, 131 (2003).
- [30] F. Bouquet, Y. Wang, I. Sheikin, T. Plackowski, A. Junod, S. Lee, and S. Tajima, Phys. Rev. Lett. 89, 257001 (2002).
- [31] Yu. G. Naidyuk, O. E. Kvitnitskaya, I. K. Yanson, S. Lee and S. Tajima, Solid State Commun. 133, 363 (2005).
- [32] Y. Bugoslavsky, Y. Miyoshi, G. K. Perkins, A. D. Caplin, L. F. Cohen, A. V. Pogrebnikov, and X. X. Xi, Phys. Rev. B 72, 224506 (2005).
- [33] A. E. Koshelev and A. A. Golubov, Phys. Rev. Lett. 90, 177002 (2004).
- [34] P. Szabo, P. Samuely, Z. Holanová, S. Bud'ko, P. C. Canfield, and J. Marcus, accepted to AIP Conference Proceedings series (LT 24), 2005.
- [35] P. Samuely, P. Szabo, J. Kacmarčík, T. Klein, Physica C 404, 460 (2004).